Eur J Nucl Med Mol Imaging (2017) 44:941–949
DOI 10.1007/s00259-017-3631-6

ORIGINAL ARTICLE

^{68}Ga-PSMA-11 PET/CT in primary staging of prostate cancer: PSA and Gleason score predict the intensity of tracer accumulation in the primary tumour

Christian Uprimny[1] · Alexander Stephan Kroiss[1] · Clemens Decristoforo[1] · Josef Fritz[2] · Elisabeth von Guggenberg[1] · Dorota Kendler[1] · Lorenza Scarpa[1] · Gianpaolo di Santo[1] · Llanos Geraldo Roig[1] · Johanna Maffey-Steffan[1] · Wolfgang Horninger[3] · Irene Johanna Virgolini[1]

Received: 3 December 2016 / Accepted: 11 January 2017 / Published online: 31 January 2017

Abstract
Purpose Prostate cancer (PC) cells typically show increased expression of prostate-specific membrane antigen (PSMA), which can be visualized by ^{68}Ga-PSMA-11 PET/CT. The aim of this study was to assess the intensity of ^{68}Ga-PSMA-11 uptake in the primary tumour and metastases in patients with biopsy-proven PC prior to therapy, and to determine whether a correlation exists between the primary tumour-related ^{68}Ga-PSMA-11 accumulation and the Gleason score (GS) or prostate-specific antigen (PSA) level.
Methods Ninety patients with transrectal ultrasound biopsy-proven PC (GS 6–10; median PSA: 9.7 ng/ml) referred for ^{68}Ga-PSMA-11 PET/CT were retrospectively analysed. PET images were analysed visually and semiquantitatively by measuring the maximum standardized uptake value (SUV_{max}). The SUV_{max} of the primary tumour and pathologic lesions suspicious for lymphatic or distant metastases were then compared to the physiologic background activity of normal prostate tissue and gluteal muscle. The SUV_{max} of the primary tumour was assessed in relation to both PSA level and GS.
Results Eighty-two patients (91.1%) demonstrated pathologic tracer accumulation in the primary tumour that exceeded physiologic tracer uptake in normal prostate tissue (median SUV_{max}: 12.5 vs. 3.9). Tumours with GS of 6, 7a (3+4) and 7b (4+3) showed significantly lower ^{68}Ga-PSMA-11 uptake, with median SUV_{max} of 5.9, 8.3 and 8.2, respectively, compared to patients with GS >7 (median SUV_{max}: 21.2; $p < 0.001$). PC patients with PSA ≥10.0 ng/ml exhibited significantly higher uptake than those with PSA levels <10.0 ng/ml (median SUV_{max}: 17.6 versus 7.7; $p < 0.001$). In 24 patients (26.7%), 82 lymph nodes with pathologic tracer accumulation consistent with metastases were detected (median SUV_{max}: 10.6). Eleven patients (12.2%) revealed 55 pathologic osseous lesions suspicious for bone metastases (median SUV_{max}: 11.6).
Conclusions The GS and PSA level correlated with the intensity of tracer accumulation in the primary tumours of PC patients on ^{68}Ga-PSMA-11 PET/CT. As PC tumours with GS 6+7 and patients with PSA values ≤10 ng/ml showed significantly lower ^{68}Ga-PSMA-11 uptake, ^{68}Ga-PSMA-11 PET/CT should be preferentially applied for primary staging of PC in patients with GS >7 or PSA levels ≥10 ng/ml.

Keywords ^{68}Ga-PSMA-11 PET/CT · Prostate cancer · Primary staging

✉ Christian Uprimny
christian.uprimny@tirol-kliniken.at

[1] Department of Nuclear Medicine, Medical University Innsbruck, Anichstrasse 35, 6020 Innsbruck, Austria

[2] Department of Medical Statistics, Informatics and Health Economics, Medical University Innsbruck, Innsbruck, Austria

[3] Department of Urology, Medical University Innsbruck, Innsbruck, Austria

Introduction

In patients with newly diagnosed prostate cancer (PC), the assessment of the exact tumour stage, in addition to prostate-specific antigen (PSA) level and Gleason score (GS) tumour grading, has major implications for prognostic grouping and choice of treatment [1, 2].

According to guidelines, magnetic resonance imaging (MRI), computed tomography (CT) and bone scintigraphy

are recommended imaging procedures for the primary staging of PC, with the choice of modality largely dependent on the risk of metastasis [1, 2]. MRI is typically applied for assessing the local tumour stage and evaluating local spread to lymph nodes (LN), whereas CT is performed both for evaluating malignant LN involvement and for detecting distant metastases [2, 3]. The use of bone scintigraphy is advised only in patients at high risk of bone metastases [1, 4].

Whole-body positron emission tomography (PET)/CT imaging using either C-11 or F-18-labelled choline has the capacity to detect both LN and distant metastases in PC patients [5–8]. Unfortunately, choline PET/CT lacks sufficient sensitivity for detecting LN metastases [6, 9, 10], and for this reason in particular, current guidelines do not recommend choline PET for standard primary staging of PC [1].

Over the past few years, the prostate-specific membrane antigen (PSMA) ligand ^{68}Ga-PSMA-11 has emerged as a promising new PET tracer in the diagnostic work-up of PC patients [11–17], showing high affinity for PSMA, a cell-surface transmembrane protein that is over-expressed in most PC cells [18–22]. In PC patients with biochemical recurrence, ^{68}Ga-PSMA-11 PET/CT has shown superiority to choline PET/CT, due to its higher accuracy, and has the potential to replace standard imaging modalities in this indication [23–25].

In primary staging of intermediate- to high-risk PC patients, ^{68}Ga-PSMA-11 PET/CT has demonstrated greater sensitivity and specificity in LN staging than conventional imaging modalities [26, 27]. However, it was also observed in these studies that some primary tumours showed no or only faintly increased ^{68}Ga-PSMA-11 uptake.

The main aim of the present study, therefore, was to test the correlation between the intensity of tracer uptake in the primary tumour and the GS and/or PSA level. This could provide the basis upon which to identify PC patients in whom the primary tumour is presumably positive on ^{68}Ga-PSMA-11 PET/CT at primary staging.

Materials and methods

Ninety patients with newly diagnosed, untreated PC who were referred for ^{68}Ga-PSMA-11 PET/CT for primary staging from January 2014 to September 2016 were analysed retrospectively. In all patients, PC was verified histologically with transrectal ultrasound (TRUS)-guided biopsy, and the GS results of TRUS biopsy served as reference for the PET findings. Patients were not strictly consecutive, as only those for which PSA values within 4 weeks prior to ^{68}Ga-PSMA-11 PET/CT imaging were available were included in the analysis. Detailed information on patient characteristics is shown in Table 1. The study was conducted according to the principles of the Declaration of Helsinki and its later amendments [28].

Table 1 Patient characteristics

Patients (n)	90
Age median (range)	64 years (47–83)
GS 6 (n)	11
GS 7a (n)[a]	30
GS 7b (n)[b]	14
GS 8 (n)	17
GS 9 (n)	13
GS 10 (n)	5
PSA median (range)	9.7 ng/ml (2.2–188.4)

GS Gleason score, *n* number

[a] GS 7a corresponds to GS 3+4

[b] GS 7b corresponds to GS 4+3

Written informed consent was obtained from all patients according to institutional guidelines.

Radiopharmaceutical

PSMA-11 (Glu-NH-CO-NH-Lys(Ahx)-HBED-CC; HBED = *N,N′*-bis[2-hydroxy-5-(carboxyethyl) benzyl]ethylenediamine-N,N′-diacetic acid) was obtained from ABX advanced biochemical compounds (Radeberg, Germany) and met Good Manufacturing Practice (GMP) quality standards. ^{68}Ga-PSMA-11 was prepared on an automated synthesis module (Modular-Lab PharmTracer; Eckert & Ziegler, Berlin) using a procedure described previously [13, 29]. The radiochemical purity of the final product was >91% as analyzed by reversed-phase high-performance liquid chromatography (HPLC) analysis and thin-layer chromatography (TLC), proving the absence of colloidal ^{68}Ga [30].

Imaging protocol

^{68}Ga-PSMA-11 PET/CT imaging was conducted using a dedicated PET/CT system (Discovery 690; GE Healthcare, Milwaukee, WI). Sixty minutes after injection of ^{68}Ga-PSMA-11 (median activity: 150 MBq; range: 78–199 MBq), a whole-body PET scan (skull base to upper thighs) was acquired in three-dimensional mode (emission time: 2 min per bed position, with an axial field of view of 15.6 cm per bed position). The variation in injected ^{68}Ga-PSMA-11 activity was due to the short half-life of ^{68}Ga and the variable elution efficiency of the ^{68}Ge/^{68}Ga radionuclide generator. However, the image quality of the PET scans in patients administered lower activity was good and was judged sufficient for accurate image analysis. Twenty-six patients (28.9%) received a diagnostic contrast-enhanced CT (ceCT) scan. The ceCT scan parameters, using GE Smart mA dose modulation, were as follows: 100 or 120 kVp, 80–450 mA, noise index 24, 0.8 s per tube rotation, slice thickness 3.75 mm and pitch 0.984. A CT

scan of the thorax, abdomen and pelvis (shallow breathing) was acquired 40–70 s after the injection of contrast agent (60–120 ml of Iomeron 400 mg/l, depending on patient body weight), followed by a CT scan of the thorax with deep-inhalation breath-hold. The relatively low number of ceCT scans reflects the fact that according to European Association of Urology (EAU) guidelines, diagnostic CT is not recommended as a standard imaging procedure in the primary staging of PC [1, 2]. In the remaining 64 patients, a low-dose CT scan was performed for attenuation correction of the PET emission data. Low-dose CT images were also used for anatomical correlation of lesions with increased uptake found on PET. The low-dose CT scan parameters, using GE Smart mA dose modulation, were as follows: 100 kVp, 15–150 mA, noise index 60, 0.8 s per tube rotation, slice thickness 3.75 mm and pitch 1.375. Reconstruction was performed with an ordered subset expectation maximization (OSEM) algorithm with four iterations/eight subsets.

Image analysis

All ^{68}Ga-PSMA PET/CT images were analysed with commercially available dedicated software (GE Advantage Workstation software version AW4.5 02), which allowed the review of PET, CT and fused imaging data in axial, coronal and sagittal slices. PET images were interpreted independently by two board-approved nuclear medicine physicians with more than 10 years of clinical experience each, who were aware of all clinical data available. Any disagreement was resolved by consensus. The site of the primary tumour within the prostate gland was known to the investigators from the TRUS biopsy. In a first step, they assessed whether the primary tumour was visually distinguishable from surrounding prostate tissue. The tumour was judged positive when tumour-related focal tracer uptake was higher than that of surrounding prostate tissue. For calculation of the maximum standardized uptake value (SUV_{max}) of the primary tumour, volumes of interest (VOIs) were drawn automatically with a manually adapted isocontour threshold centred on lesions with focally increased uptake corresponding to the tumour site verified by TRUS biopsy. In cases where the primary tumour could not be clearly identified on PET images, VOIs were placed over the area where the primary tumour was found in TRUS biopsy. With respect to the evaluation of LN and distant metastases, any focal uptake higher than surrounding background activity that did not correspond to physiologic tracer accumulation was considered pathologic and suggestive of malignancy. This interpretation criterion is the result of our clinical experience and is in line with published literature [13, 14, 31]. A quantitative cut-off for PC lesions has not been described do date. The SUV_{max} values of metastases were calculated within VOIs placed over the sites of pathologic tracer accumulation consistent with tumour lesions. In addition, the SUV_{max} was measured in areas with physiologic tracer uptake in normal prostate tissue (BGp) and in the gluteal muscle (BGm). SUV_{max} was chosen because SUV_{mean} depends on the volume of interest drawn by the investigator, whereas SUV_{max} is operator-independent [11].

Statistical analysis

Associations between the GS and PSA and the SUV_{max} of the primary tumour were described descriptively (Crosstabs; Spearman correlation coefficient r_S), visualized in scatter plots, and evaluated using the Mann–Whitney U test and Kruskal–Wallis test. Methods appropriate for (right-)skewed data (such as SUV_{max}) were selected. A significance level of $\alpha = 0.05$ (two-tailed) was applied. Statistical analyses were performed using SPSS version 22.0 software (IBM Corp., Armonk, NY).

Results

The GS among patients ranged from 6 to 10; patients presented with a median PSA value of 9.7 ng/ml (see also Table 1). In 82 of 90 patients (91.1%), the primary tumour was able to be visualized on ^{68}Ga-PSMA-11 PET/CT, whereas in eight patients (8.9%), the primary tumour was not distinguishable from the surrounding prostate tissue (for an example of a patient without visualization of the primary tumour, see Fig. 1). The median SUV_{max} among all tumours was 11.5 (range: 2.7–66.4), compared to a median SUV_{max} of 3.9 (range: 2.5–6.6) and 1.2 (range: 0.8–2.0) in normal prostate tissue and gluteal muscle, respectively. The median SUV_{max} of tumours judged as positive was significantly higher than that in tumours not visible on ^{68}Ga-PSMA-11 PET/CT (12.5 versus 3.6; $p < 0.001$). Eighty-three tumours (92.2%) showed a higher SUV_{max} than the median SUV_{max} of normal prostate tissue, whereas 65 primary tumours (72.2%) presented a higher median SUV_{max} than the maximum SUV_{max} measured in normal prostate tissue (max SUV_{max}: 6.6).

All primary tumours rated negative belonged to the subgroups GS 6 ($n = 3$), GS 7a ($n = 4$) or GS 7b ($n = 1$). All tumours of subgroups GS 8–10 exhibited higher ^{68}Ga-PSMA-11 accumulation than surrounding prostate tissue. Combining GS and tumour-related tracer uptake, lower median SUV_{max} values were found for the subgroups GS 6 (SUV_{max}: 5.9), GS 7a (SUV_{max}: 8.3) and GS 7b (SUV_{max}: 8.2) than for GS 8 (SUV_{max}: 21.2), GS 9 (SUV_{max}: 22.8) and GS 10 (SUV_{max}: 17.7). Differences in median SUV_{max} values between tumours with GS of 6, 7a and 7b and those with GS of 8, 9 and 10 were statistically significant ($p < 0.001$ and $p = 0.005$, respectively). A comparison of GS subgroups and SUV_{max} values for all tumours and normal prostate tissue is illustrated in Fig. 2, and detailed information about the results and the values of

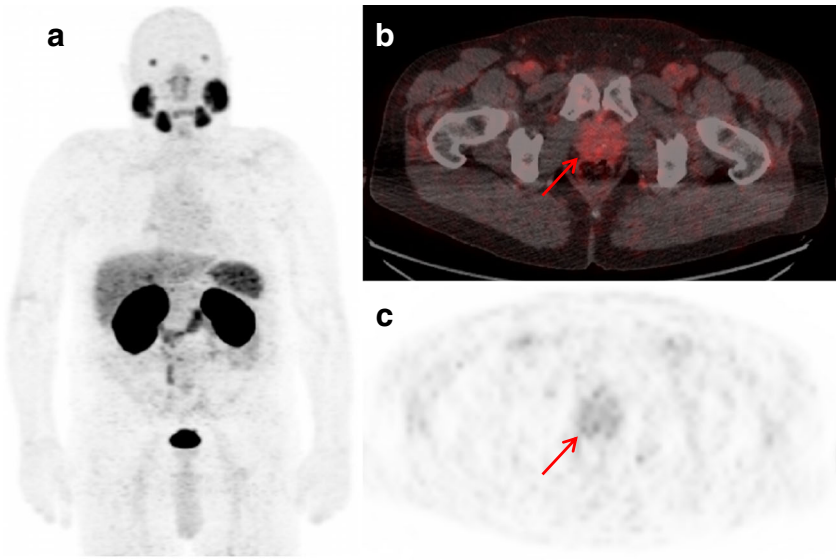

Fig. 1 ^{68}Ga-PSMA-11 PET/CT with maximum-intensity projection (**a**), fused PET/CT (**b**) and axial PET (**c**) images of a 64-year-old patient with biopsy-proven PC (GS 3+4) and a PSA value of 3.3 ng/ml. On fused PET/CT images and PET images alone, no pathologic tracer uptake exceeding tracer uptake in normal prostate tissue at the site of the primary tumour was detected (*red arrow* pointing to tumour area known from TRUS-guided biopsy). The SUV_{max} of the primary tumour was 2.9, compared to a maximum SUV_{max} of 3.3 in normal prostate tissue

the subgroups is listed in Table 2. A comparison of median SUV_{max} between the subgroups with GS 7a and 7b did not detect a statistically significant difference (8.3 vs. 8.2; $p = 1.0$).

With respect to PSA values, the median PSA levels of patients with tumours that were not visible did not differ significantly from those with identifiable primary tumours (median PSA: 6.1 vs. 10.0 ng/ml; $p < 0.035$). The PSA values and corresponding SUV_{max} values of the primary tumours for all patients are shown in Fig. 3. ^{68}Ga-PSMA-11 uptake in the primary tumour was higher in patients with PSA levels ≥10 ng/ml than those with PSA values <10 ng/ml, exhibiting a median SUV_{max} of 7.7 vs. 17.6, respectively, and resulting in a statistically significant difference ($p < 0.001$), as shown in Table 3. In the GS 7a and GS 7b subgroups, the median SUV_{max} was higher in patients with PSA levels ≥10 ng/ml versus <10 ng/ml (6.8 vs. 10.6 with GS 7a, and 7.5 vs. 19.0 with GS 7b; see Table 4). However, the difference was statistically significant only in subgroup 7a ($p = 0.036$), and did not reach statistical significance in group GS 7b ($p = 0.054$).

In addition, the SUV_{max} values for patients in whom radical prostatectomy was performed were compared to definitive postoperative histology results ($n = 49$), which revealed a statistically significant correlation ($p < 0.001$) between the median SUV_{max} and GS: a median SUV_{max} of 6.8 in the group with GS of 6 and 7 (range: 2.7–35.1), and a median SUV_{max} of 19.5 in GS 8–10 tumours (range: 5.3–65).

As for the detection of metastases, in 24 patients (26.7%), a total of 82 LN with pathologic ^{68}Ga-PSMA-11 uptake consistent with metastases were detected, with a median SUV_{max} of 10.6 (range: 3.1–90.6) and a median diameter of 10.9 mm (range: 3.9–32.9). The median SUV_{max} of tumours in patients with LN metastases was higher than in patients without malignant LN involvement (18.7 vs. 9.7), also reaching statistical significance ($p = 0.001$).

The histologic results of pelvic LN dissection were available in 49 patients. Among 18 patients who showed LN metastases on histologic evaluation, 11 patients exhibited LN

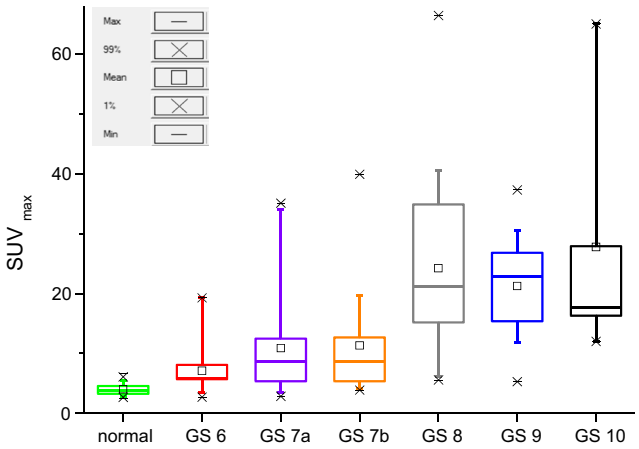

Fig. 2 Comparison of ^{68}Ga-PSMA-11 uptake expressed in SUV_{max} values in normal prostate tissue (*green box*) and in primary tumours of different GS subgroups. Box plots demonstrate that median SUV_{max} is significantly higher in tumours with GS >7 (8, 9, 10) than in primary tumours with GS of 6, 7a (3+4) and 7b (4+3)

Table 2 SUV_{max} values of different Gleason score subgroups

	N	Median SUV_{max}	Mean SUV_{max}	SD SUV_{max}	Range SUV_{max}
GS 6	11	5.9	7.1	4.6	2.7–19.3
GS 7a	30	8.3	10.9	8.2	2.9–35.1
GS 7b	14	8.2	11.3	9.6	3.9–40.0
GS 8	17	21.2	24.2	15.5	5.6–66.4
GS 9	13	22.8	21.3	8.9	5.3–37.3
GS 10	5	17.7	27.8	21.6	12.0–65.0
Total	90	11.5	15.5	12.6	2.7–66.4

N number, *SD* standard deviation, *GS* Gleason score

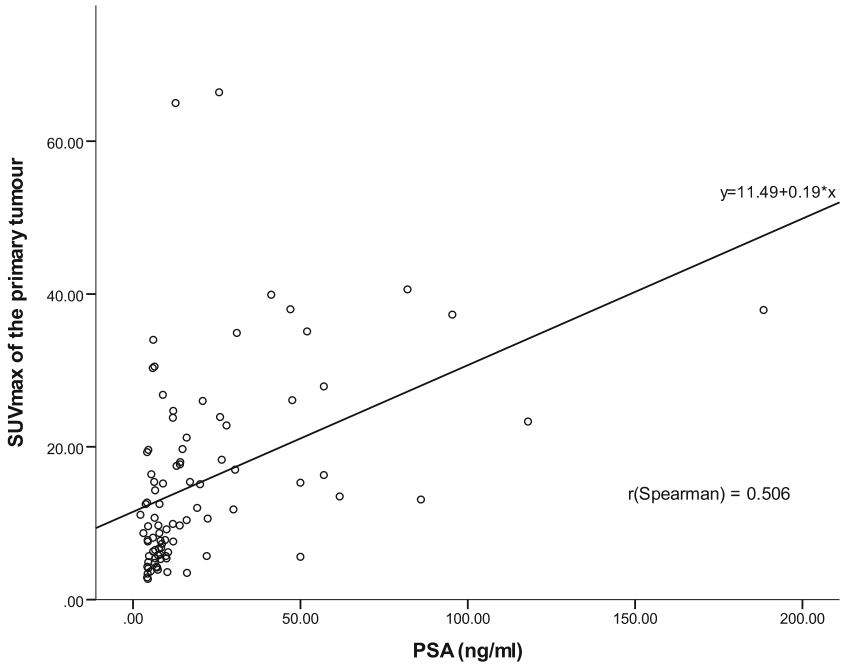

Fig. 3 Comparison of PSA values and primary tumour-related ^{68}Ga-PSMA-11 uptake, expressed as SUV_{max}. Scatter plot shows the correlation between PSA level and median SUV_{max} value for tumours, which reaches statistical significance ($r_{Spearman} = 0.506$; $p < 0.001$)

with pathologic ^{68}Ga-PSMA-11 accumulation. In two patients with PET-positive LN, malignant LN spread could not be confirmed on histologic exam. In patient-based analysis, the calculated sensitivity and specificity were 61.1 and 90.0%, respectively.

In total, 56 lesions with pathologic tracer accumulation suspicious for distant metastases were found in 11 patients (12.2%). All but one were limited to the bone, exhibiting a median SUV_{max} of 11.6 (range: 2.6–82.6). Most of the bone lesions showed a correlate on CT images. Sclerotic alterations were detected in 41 lesions, and four lesions corresponded with an osteolytic lesion on CT. Ten pathologic osseous foci showed no pathologic finding on CT, although the median SUV_{max} was higher in these lesions than in bone lesions also positive on CT (14.2 vs. 10.1). CT images served as reference for malignant bone involvement in all lesions that showed a clear correlate on ceCT or on low-dose CT ($n = 45$). In four ^{68}Ga-PSMA-11-positive lesions not visible on CT, metastases were confirmed with MRI. Six lesions not discernible on CT were not further investigated, as they were present in two patients who also showed sclerotic metastases, rendering malignant bone infiltration in these cases very likely (an example of a patient with both PET-positive bone metastases visible on CT and no correlation on CT images is presented in Fig. 4). SUV_{max} values for all metastases are listed in Table 5. In one patient, a pathologic lesion with increased tracer accumulation (SUV_{max}: 8) highly suspicious for PC metastasis was found in the lung, but histologic verification revealed a metastasis of a renal cell carcinoma.

The median SUV_{max} of primary tumours with distant metastases was higher than the median SUV_{max} for patients in whom no distant metastases were found (17.7 vs. 10.5), although the difference was not statistically significant ($p = 0.098$). The median PSA value for patients judged positive for distant metastases was significantly higher than in patients with no sign of distant metastases (30.0 vs. 8.19 ng/ml; $p = 0.001$); the same was true for patients with LN metastases versus patients without LN metastases (22.29 vs. 7.87 ng/ml; $p < 0.001$), as is also presented in Table 6.

Table 3 Comparison of PSA level and SUV_{max} of primary tumours between patients with PSA < 10 ng/ml and those with PSA ≥ 10 ng/ml

PSA (ng/ml)	N	Median SUV_{max}	Mean SUV_{max}	SD SUV_{max}	Range SUV_{max}
<10	46	7.7	10.2	7.6	2.7–34.0
≥10	44	17.6	21.0	14.4	3.5–66.4

N number, *SD* standard deviation

Table 4 Comparison of subgroups GS 7a and GS 7b with PSA values < 10 ng/ml and ≥ 10 ng/ml, respectively, in relation to SUV_{max} values of primary tumours

	N	Median SUV_{max}	Mean SUV_{max}	SD SUV_{max}	Range SUV_{max}
GS 7a and PSA < 10 ng/ml	21	6.8	9.1	6.8	2.9–34.0
GS 7a and PSA ≥ 10 ng/ml	9	10.6	15.0	10.6	5.4–35.1
GS 7b and PSA < 10 ng/ml	10	7.5	7.5	7.5	3.9–12.7
GS 7b and PSA ≥ 10 ng/ml	4	19.0	20.9	8.3	5.7–39.9

N number, *SD* standard deviation

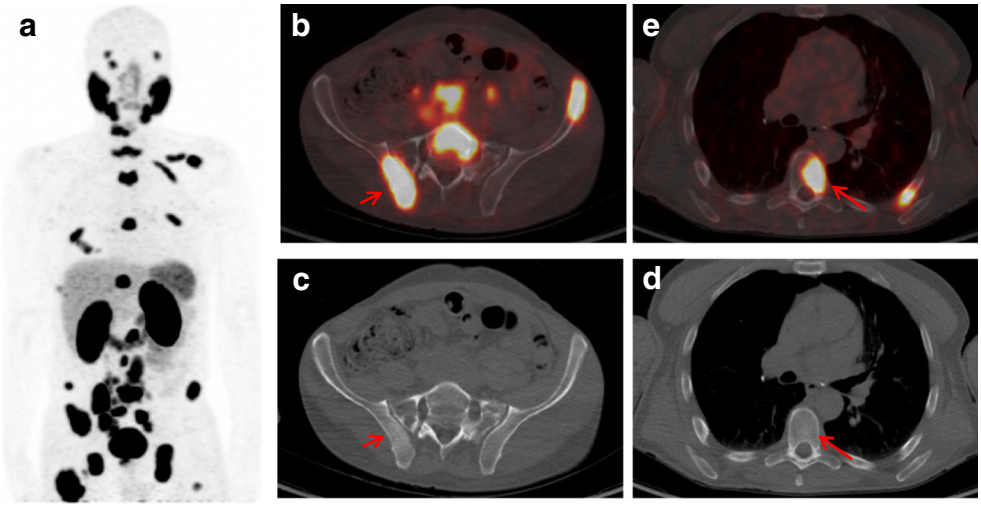

Fig. 4 ^{68}Ga-PSMA-11 PET/CT with maximum-intensity projection (MIP) (**a**), fused PET/CT (**b**, **e**) and CT (**c**, **d**) images of a 71-year-old PC patient with biopsy-proven PC (GS 3+4) and a PSA value of 3.3 ng/ml: MIP shows multiple bone metastases. The bone metastasis in the right iliac bone (*short red arrow*) shows intense tracer accumulation, with an SUV_{max} value of 26.1 on fused PET/CT image (**b**) corresponding to a faint sclerotic area on CT image (**c**). In contrast, the bone metastasis in the thoracic spine (*long red arrow*) with high tracer uptake (SUV_{max}: 23.8) displayed on fused PET/CT (**e**) does not show a pathologic correlate on CT (d), and probably constitutes malignant bone marrow infiltration

Discussion

The main aim of our retrospective study was to determine whether a correlation exists between the intensity of ^{68}Ga-PSMA-11 accumulation in the primary tumours of PC patients and the GS and/or PSA value. In addition, we sought to ascertain whether stratification of PC patients and predicting PET positivity of the primary tumour would be possible using these parameters.

PC cells typically show increased expression of PSMA, enabling targeted PET imaging with PSMA ligands, among which ^{68}Ga-PSMA-11 has demonstrated high affinity for PSMA [18, 29, 32–34]. Benign prostatic epithelium also exhibits enhanced PSMA expression, as proved by immunohistochemical studies; however, the intensity of expression is lower than that in prostate cancer cells [20–22]. On ^{68}Ga-PSMA-11 PET/CT, increased uptake of ^{68}Ga-PSMA-11 in normal prostate tissue has been described in previous studies, with a median SUV_{max} value ranging from 2.4 to 5.5, and the highest median SUV_{max} of 8.3 on PET imaging 60 min after tracer injection [11, 34, 35]. Our data are similar, and more or less confirm these values, as our patients showed a median SUV_{max} of 3.9 in normal prostate tissue and a maximum SUV_{max} of 6.6.

With respect to the diagnostic work-up of prostate cancer patients, in patients with biochemical recurrence, ^{68}Ga-PSMA-11 PET appears to be superior to choline PET, due to the higher accuracy of the former compared to choline PET/CT [13, 17, 23–25].

Promising data have also been reported for primary staging, with ^{68}Ga-PSMA-11 PET/CT showing higher sensitivity and specificity, at least for nodal staging, compared to both CT and choline PET/CT [26, 34, 35]. In a series of 130 patients with intermediate- to high-risk PC staged with ^{68}Ga-PSMA-11 PET/CT, Maurer et al. observed that 8.4% of primary tumours showed no increase or only a slight increase in tracer accumulation. In another study, Budäus et al. reported that 7.1% of primary tumours were negative on ^{68}Ga-PSMA-11 PET/CT [27]. This is in line with our findings, as 8.9% of primary tumours were not distinguishable from the surrounding normal prostate tissue. However, whilst 82 primary tumours (91.1%) showed a median SUV_{max} higher than that

Table 5 SUV_{max} values of lymph node and bone metastases

	N	Median SUV_{max}	Mean SUV_{max}	SD SUV_{max}	Range SUV_{max}
LN metastases	82	10.6	15.8	15.0	3.1–90.6
Bone metastases	55	11.6	15.9	13.7	2.6–82.6
CT-positive BM	45	10.1	15.0	7.9	6.4–29.7
CT-negative BM	10	14.2	15.0	15.0	2.6–82.6

BM bone metastases, *N* number, *SD* standard deviation

Table 6 SUV_{max} values of primary tumour and PSA level in subgroups of patients with and without metastases

	LN pos. ($n = 66$)	LN neg. ($n = 24$)	BM pos. ($n = 11$)	BM neg. ($n = 79$)
Median SUV_{max} tumour	18.7	9.7	17.7	10.5
SUV_{max} tumour range	4.9–66.4	2.7–38.0	5.6–39.9	2.7–66.4
Median PSA (ng/ml)	20.72	8.00	30.00	8.19

BM bone metastases

of normal prostate tissue, only 65 primary tumours (72.2%) presented with a median SUV_{max} higher than the maximum SUV_{max} measured in normal prostate tissue (maximum SUV_{max}: 6.6). Hence, in addition to tumours that are completely indiscernible on ^{68}Ga-PSMA-11 PET/CT, there are obviously tumours that show only a faint increase in tracer uptake compared with normal prostate tissue. Clearly, in these cases, detection of the primary tumour will be challenging.

Metastases of primary tumours with relatively low ^{68}Ga-PSMA-11 accumulation may also be missed. With respect to the detection of LN metastases, Maurer et al. demonstrated higher sensitivity with ^{68}Ga-PSMA-11 PET than with conventional imaging alone (68.3 vs. 28.2% in a template-based analysis). Histologically verified LN metastases that were not positive on ^{68}Ga-PSMA-11 PET/CT were either too small to detect or were metastases of primary tumours in which tracer uptake was absent or low. When patients with primary tumours negative on ^{68}Ga-PSMA-11 PET were excluded, sensitivity increased to 78.2%.

In general, sufficient tracer uptake in the primary tumour is considered a precondition for visualisation and detection of metastases on PET imaging. The use of ^{68}Ga-PSMA-11 PET/CT as a staging procedure should be reserved for PC patients with a high likelihood of marked PET positivity of the primary tumour. It would be useful to have parameters at the initial diagnosis of PC that could predict whether a primary tumour is suitable for imaging with ^{68}Ga-PSMA-11 PET/CT. This issue was addressed in part in a recently published study by Sachpekides et al. [35]. In 24 patients with PC referred to ^{68}Ga-PSMA-11 PET/CT for primary staging, the authors found a weak to moderate statistically significant correlation between PSA value/GS and tracer accumulation in tumour lesions. Besides the fact that the main aim of this study was the assessment of tracer pharmacokinetics on dynamic PET/CT, a major limitation of the study was the relatively small number of patients. In addition, patients with GS of 6 and 10 were not investigated, and no GS information was available or three patients. For this reason, we wanted to verify these promising results in a larger cohort of patients that included tumours with GS of 6 and 10 and that allowed us to perform subgroup analysis with higher statistical power.

With regard to the correlation between GS and ^{68}Ga-PSMA-11 uptake in the primary tumour, our data support the observation reported by Sachpekides et al. Tumours with GS of 6, 7a and 7b exhibited a statistically significant lower ^{68}Ga-PSMA-11 accumulation than tumours with GS of 8, 9 and 10, based on the median SUV_{max}. To account for the different clinical behaviour of GS 3+4 (7a) and GS 4+3 (7b), we sought to determine whether these two groups differed in ^{68}Ga-PSMA-11 uptake. However, tracer uptake of the primary tumour was almost identical, with a median SUV_{max} of 8.3 and 8.2, respectively ($p = 1.000$).

Combining GS and PSA for comparison with tumour-related tracer accumulation in both GS 7a and GS 7b subgroups, the median SUV_{max} was higher in patients with PSA levels ≥10 ng/ml than those with PSA values <10 ng/ml (6.8 vs. 10.6 with GS 7a, and 7.5 vs. 19.0 with GS 7b). However, the difference was statistically significant only in subgroup 7a ($p = 0.036$), and despite a marked difference in absolute values in patients with GS 7b, it did not reach statistical significance ($p = 0.054$), likely due to the relatively low number of patients in this subgroup.

As TRUS-biopsy results served as reference in the above-mentioned patients, we performed an additional analysis in a subgroup of patients for whom postoperative histology of the primary tumour after radical prostatectomy was available ($n = 49$). Again, a statistically significant difference in median SUV_{max} values was observed between GS 6/7 and GS 8–10 tumours (SUV_{max}: 6.8 vs. 19.5; $p < 0.001$).

The correlation between PSA value and positive findings on ^{68}Ga-PSMA-11 PET/CT is well demonstrated in PC patients with biochemical relapse [12, 13]. As the PSA level in this setting largely reflects tumour volume, the sensitivity of ^{68}Ga-PSMA-11 PET/CT in detecting recurrent lesions increases as PSA values increase. In primary staging of PC, Sachkepides et al. found a statistically significant correlation between PSA value and SUV_{max} of primary tumours [35]. Our results corroborate these findings, as patients with higher PSA levels exhibited statistically significant higher tracer uptake in the primary tumour. Importantly, the PSA levels of patients with primary tumours not visible on ^{68}Ga-PSMA-11 PET/CT were significantly lower than those in patients with PET-positive tumours (median PSA: 6.1 vs. 10.0 ng/ml; $p < 0.035$). Given the clinical impact, we additionally compared primary tumour-related tracer accumulation in patients with PSA values <10 ng/ml to those with PSA-values ≥10 ng/ml, and found a statistically relevant difference as well (median SUV_{max}: 7.7 vs. 17.6; $p < 0.001$;). And although it was not the main aim of our study, we also assessed the detection rate of lesions with pathologic ^{68}Ga-PSMA-11 uptake consistent with metastases. In 26.7% of patients, a total of 82 LN with pathologic tracer uptake suspicious for malignant involvement were found, with a median SUV_{max} of 10.6 (range: 3.1–90.6), which was markedly higher than the physiologic background activity of the gluteal muscle (median SUV_{max}: 1.2). It is worth noting that the median SUV_{max} of primary tumours with pathologic LN on ^{68}Ga-PSMA-11 PET/CT was significantly higher than that in tumours without suspicion of LN metastases on PET/CT images (18.7 vs. 9.7; $p < 0.001$).

Although it was not the primary purpose of our study, we also compared PET findings of LN with postoperative histology in 49 patients in whom pelvic LN dissection was performed. In a patient-based analysis of the detection of LN metastases with ^{68}Ga-PSMA-11 PET/CT, sensitivity and

specificity of 61.1 and 90.0% were found, respectively. Similar results were described by Maurer et al. in a study including 130 patients [26]. However, in contrast to that study, we were unable to conduct a template-based analysis, as no standardized bilateral template pelvic LN dissection was performed to confirm the findings of ^{68}Ga-PSMA-11 PET/CT. This has been investigated in previous studies with at least somewhat promising results with respect to the sensitivity for detecting LN metastases [26, 27, 36–38], demonstrating in particular a higher detection rate for LN metastases with ^{68}Ga-PSMA-11 PET compared with choline PET [25, 39].

With regard to the detection of distant metastases, 55 bone lesions with pathologic ^{68}Ga-PSMA-11 accumulation highly suspicious for metastases were detected in 11 patients (12.2%). Bone lesions in most cases were clearly visible on PET images due to excellent lesion-to-background contrast, exhibiting a median SUV_{max} of 11.6. The majority of pathologic foci judged positive in PET displayed a pathologic correlate on CT images (41 sclerotic lesions, 4 osteolytic lesions). However, pathologic bone foci were also detected that were negative on CT ($n = 10$). One possible reason for this finding is that in some cases, only low-dose CT was performed, with the possibility of missing discrete bone alterations. On the other hand, these cases may represent malignant bone marrow infiltration with no reaction of the bone visible on CT images. Interestingly, the median SUV_{max} of these bone lesions not visible on CT was higher than that in osteoblastic/osteolytic lesions (14.2 vs. 10.1). At least in osteoblastic lesions, this can be partially explained by lower tumour volume in sclerotic areas. Figure 4 depicts a case of multiple bone metastases with PET-positive sclerotic bone metastases and osseous lesions with intense ^{68}Ga-PSMA-11 uptake, without a correlate on CT. Also of note was the association between the intensity of tracer accumulation in the primary tumour and the presence of pathologic osseous foci, with a median SUV_{max} of 17.7 vs. 10.5 for the primary tumour for bone-positive and bone-negative patients, respectively.

A major limitation of our study is the retrospective nature of the analysis. Although we acknowledge that further validation of our findings with prospective trials is required, the data in our relatively large patient cohort are quite consistent.

Conclusions

In the years since ^{68}Ga-PSMA-11 PET/CT was introduced for the primary staging of PC, various studies have observed that primary tumours may show varying intensity of ^{68}Ga-PSMA-11 uptake, with tumours sometimes not distinguishable from surrounding normal prostate tissue.

In the present study, we demonstrated that the intensity of tumour-related tracer uptake on ^{68}Ga-PSMA-11 PET/CT correlates with PSA level and GS in newly diagnosed PC. Based on our findings, we recommend that ^{68}Ga-PSMA-11 PET/CT for the primary staging of PC be preferentially performed in tumours with GS > 7 or patients with PSA level ≥10 ng/ml, whereas staging with ^{68}Ga-PSMA-11 PET/CT in tumours with GS of 6 and 7 with PSA values <10 ng/ml is not advisable, taking into account the significantly lower ^{68}Ga-PSMA uptake in these tumours.

Acknowledgments We want to express our gratitude to all the members of our PET staff for their contribution in performing this study.

Compliance with ethical standards

Conflict of interest All authors declare that they have no conflict of interest.

Ethical approval All procedures performed in this study were in accordance with the ethical standards of the institutional and national research committee and with the principles of the 1964 Declaration of Helsinki and its later amendments or comparable ethical standards. All patients published in this manuscript provided written informed consent.

References

1. Mottet N, Bellmunt J, Bolla M, Briers E, Cumberbatch MG, De Santis M, et al. EAU-ESTRO-SIOG Guidelines on Prostate Cancer. Part 1: screening, diagnosis, and local treatment with curative intent. Eur Urol. 2016. doi:10.1016/j.eururo.2016.08.003.
2. Heidenreich A, Bastian PJ, Bellmunt J, Bolla M, Joniau S, van der Kwast T, et al. EAU guidelines on prostate cancer: Part 1: screening, diagnosis, and local treatment with curative intent-update 2013. Eur Urol. 2014;65(1):124–37.
3. de Rooij M, Hamoen EH, Witjes JA, Barentsz JO, Rovers MM. Accuracy of magnetic resonance imaging for local staging of prostate cancer: a diagnostic meta-analysis. Eur Urol. 2016;70(2):233–45. doi:10.1016/j.eururo.2015.07.029.
4. Zacho HD, Barsi T, Mortensen JC, Bertelsen H, Petersen LJ. Validation of contemporary guidelines for bone scintigraphy in prostate cancer staging: a prospective study in patients undergoing radical prostatectomy. Scand J Urol. 2016;50(1):29–32.
5. Beheshti M, Langsteger W. PET imaging of prostate cancer using radiolabeled choline. PET Clin. 2009;4(2):173–84. doi:10.1016/j.cpet.2009.06.003.
6. Evangelista L, Briganti A, Fanti S, Joniau S, Reske S, Schiavina R, et al. New clinical indications for (18)F/(11)C-choline, new tracers for positron emission tomography and a promising hybrid device for prostate cancer staging: a systematic review of the literature. Clin Nucl Med. 2016;41(9):746.
7. Fanti S, Minozzi S, Castellucci P, Balduzzi S, Herrmann K, Krause BJ, et al. PET/CT with (11)C-choline for evaluation of prostate cancer patients with biochemical recurrence: meta-analysis and critical review of available data. Eur J Nucl Med Mol Imaging. 2016;43(1):55–69. doi:10.1007/s00259-015-3202-7.
8. Ceci F, Herrmann K, Castellucci P, Graziani T, Bluemel C, Schiavina R, et al. Impact of 11C-choline PET/CT on clinical decision making in recurrent prostate cancer: results from a retrospective two-centre trial. Eur J Nucl Med Mol Imaging. 2014;41(12):2222–31. doi:10.1007/s00259-014-2872-x.
9. Picchio M, Briganti A, Fanti S, Heidenreich A, Krause BJ, Messa C, et al. The role of choline positron emission tomography/computed tomography in the management of patients with prostate-specific antigen progression after radical treatment of

prostate cancer. Eur Urol. 2011;59(1):51–60. doi:10.1016/j.eururo.2010.09.004.
10. Kitajima K, Murphy RC, Nathan MA, Sugimura K. Update on positron emission tomography for imaging of prostate cancer. Int J Urol. 2014;21(1):12–23. doi:10.1111/iju.12250.
11. Afshar-Oromieh A, Malcher A, Eder M, Eisenhut M, Linhart HG, Hadaschik BA, et al. PET imaging with a [68Ga]gallium-labelled PSMA ligand for the diagnosis of prostate cancer: biodistribution in humans and first evaluation of tumour lesions. Eur J Nucl Med Mol Imaging. 2013;40(4):486–95. doi:10.1007/s00259-012-2298-2.
12. Afshar-Oromieh A, Avtzi E, Giesel FL, Holland-Letz T, Linhart HG, Eder M, et al. The diagnostic value of PET/CT imaging with the (68)Ga-labelled PSMA ligand HBED-CC in the diagnosis of recurrent prostate cancer. Eur J Nucl Med Mol Imaging. 2015;42(2):197–209. doi:10.1007/s00259-014-2949-6.
13. Ceci F, Uprimny C, Nilica B, Geraldo L, Kendler D, Kroiss A, et al. (68)Ga-PSMA PET/CT for restaging recurrent prostate cancer: which factors are associated with PET/CT detection rate? Eur J Nucl Med Mol Imaging. 2015;42(8):1284–94. doi:10.1007/s00259-015-3078-6.
14. Eiber M, Maurer T, Souvatzoglou M, Beer AJ, Ruffani A, Haller B, et al. Evaluation of Hybrid ^{68}Ga-PSMA Ligand PET/CT in 248 patients with biochemical recurrence after radical prostatectomy. J Nucl Med. 2015;56(5):668–74. doi:10.2967/jnumed.115.154153.
15. Lindenberg L, Choyke P, Dahut W. Prostate cancer imaging with novel PET tracers. Curr Urol Rep. 2016;17(3):18. doi:10.1007/s11934-016-0575-5.
16. Jadvar H. PSMA PET, in Prostate Cancer. J Nucl Med. 2015;56(8):1131–2. doi:10.2967/jnumed.115.157339.
17. Perera M, Papa N, Christidis D, Wetherell D, Hofman MS, Murphy DG, et al. Sensitivity, specificity, and predictors of positive 68Ga-prostate-specific membrane antigen positron emission tomography in advanced prostate cancer: a systematic review and meta-analysis. Eur Urol. 2016. doi:10.1016/j.eururo.2016.06.021.
18. Banerjee SR, Pullambhatla M, Byun Y, Nimmagadda S, Green G, Fox JJ, et al. 68Ga-labeled inhibitors of prostate-specific membrane antigen (PSMA) for imaging prostate cancer. J Med Chem. 2010;53(14):5333–41.
19. Ghosh A, Heston WD. Tumor target prostate specific membrane antigen (PSMA) and its regulation in prostate cancer. J Cell Biochem. 2004;91(3):528–39.
20. Sweat SD, Pacelli A, Murphy GP, Bostwick DG. Prostate-specific membrane antigen expression is greatest in prostate adenocarcinoma and lymph node metastases. Urology. 1998;52(4):637–40.
21. Bostwick DG, Pacelli A, Blute M, Roche P, Murphy GP. Prostate specific membrane antigen expression in prostatic intraepithelial neoplasia and adenocarcinoma: a study of 184 cases. Cancer. 1998;82(11):2256–61.
22. Silver DA, Pellicer I, Fair WR, Heston WD, Cordon-Cardo C. Prostate-specific membrane antigen expression in normal and malignant human tissues. Clin Cancer Res. 1997;3(1):81–5.
23. Afshar-Oromieh A, Haberkorn U, Eder M, Eisenhut M, Zechmann CM. [68Ga]Gallium-labelled PSMA ligand as superior PET tracer for the diagnosis of prostate cancer: comparison with 18F-FECH. Eur J Nucl Med Mol Imaging. 2012;39(6):1085–6. doi:10.1007/s00259-012-2069-0.
24. Morigi JJ, Stricker PD, van Leeuwen PJ, Tang R, Ho B, Nguyen Q, et al. Prospective comparison of 18F-fluoromethylcholine versus 68Ga-PSMA PET/CT in prostate cancer patients Who have rising PSA after curative treatment and Are being considered for targeted therapy. J Nucl Med. 2015;56(8):1185–90. doi:10.2967/jnumed.115.160382.
25. Afshar-Oromieh A, Zechmann CM, Malcher A, Eder M, Eisenhut M, Linhart HG, et al. Comparison of PET imaging with a (68)Ga-labelled PSMA ligand and (18)F-choline-based PET/CT for the diagnosis of recurrent prostate cancer. Eur J Nucl Med Mol Imaging. 2014;41(1):11–20. doi:10.1007/s00259-013-2525-5.
26. Maurer T, Gschwend JE, Rauscher I, Souvatzoglou M, Haller B, Weirich G, et al. Diagnostic efficacy of (68)gallium-PSMA positron emission tomography compared to conventional imaging for lymph node staging of 130 consecutive patients with intermediate to high risk prostate cancer. J Urol. 2016;195(5):1436–43. doi:10.1016/j.juro.2015.12.025.
27. Budäus L, Leyh-Bannurah SR, Salomon G, Michl U, Heinzer H, Huland H, et al. Initial experience of (68)Ga-PSMA PET/CT imaging in high-risk prostate cancer patients prior to radical prostatectomy. Eur Urol. 2016;69(3):393–6. doi:10.1016/j.eururo.2015.06.010.
28. World Medical Association Declaration of Helsinki: ethical principles for medical research involving human subjects. JAMA. 2000;284:3043–5.
29. Mueller D, Klette I, Baum RP, Gottschaldt M, Schultz MK, Breeman WA. Simplified NaCl based (68)Ga concentration and labeling procedure for rapid synthesis of (68)Ga radiopharmaceuticals in high radiochemical purity. Bioconjug Chem. 2012;23(8):1712–7. doi:10.1021/bc300103t.
30. Eder M, Neels O, Müller M, Bauder-Wüst U, Remde Y, Schäfer M, et al. Novel preclinical and radiopharmaceutical aspects of [68Ga]Ga-PSMA-HBED-CC: a new PET tracer for imaging of prostate cancer. Pharmaceuticals (Basel). 2014;7(7):779–96.
31. Rauscher I, Maurer T, Fendler WP, Sommer WH, Schwaiger M, Eiber M. (68)Ga-PSMA ligand PET/CT in patients with prostate cancer: how we review and report. Cancer Imaging. 2016;16(1):14. doi:10.1186/s40644-016-0072-6. Review.
32. Schäfer M, Bauder-Wüst U, Leotta K, Zoller F, Mier W, Haberkorn U, et al. A dimerized urea-based inhibitor of the prostate-specific membrane antigen for 68Ga-PET imaging of prostate cancer. EJNMMI Res. 2012;2(1):23. doi:10.1186/2191-219X-2-23.
33. Eder M, Schäfer M, Bauder-Wüst U, Hull WE, Wängler C, Mier W, et al. 68Ga-complex lipophilicity and the targeting property of a urea-based PSMA inhibitor for PET imaging. EJNMMI Res. 2012;2(1):23. doi:10.1186/2191-219X-2-23.
34. Demirci E, Sahin OE, Ocak M, Akovali B, Nematyazar J, Kabasakal L. Normal distribution pattern and physiological variants of 68Ga-PSMA-11 PET/CT imaging. Nucl Med Commun. 2016;37(11):1169–79. doi:10.1097/MNM.0000000000000566.
35. Sachpekidis C, Kopka K, Eder M, Hadaschik BA, Freitag MT, Pan L, et al. 68Ga-PSMA-11 dynamic PET/CT imaging in primary prostate cancer. Clin Nucl Med. 2016;41(11):e473–9.
36. Herlemann A, Wenter V, Kretschmer A, Thierfelder KM, Bartenstein P, Faber C, et al. 68Ga-PSMA positron emission tomography/computed tomography provides accurate staging of lymph node regions prior to lymph node dissection in patients with prostate cancer. Eur Urol. 2016. doi:10.1016/j.eururo.2015.12.051.
37. Kabasakal L, Demirci E, Ocak M, Akyel R, Nematyazar J, Aygun A, et al. Evaluation of PSMA PET/CT imaging using a 68Ga-HBED-CC ligand in patients with prostate cancer and the value of early pelvic imaging. Nucl Med Commun. 2015;36(6):582–7. doi:10.1097/MNM.0000000000000290.
38. Sahlmann CO, Meller B, Bouter C, Ritter CO, Ströbel P, Lotz J, et al. Biphasic ^{68}Ga-PSMA-HBED-CC-PET/CT in patients with recurrent and high-risk prostate carcinoma. Eur J Nucl Med Mol Imaging. 2016;43(5):898–905. doi:10.1007/s00259-015-3251-y.
39. Schwenck J, Rempp H, Reischl G, Kruck S, Stenzl A, Nikolaou K, et al. Comparison of 68Ga-labelled PSMA-11 and 11C-choline in the detection of prostate cancer metastases by PET/CT. Eur J Nucl Med Mol Imaging. 2016.